An *ab initio* molecular dynamics study of water–carbon tetrachloride liquid–liquid interface: nature of interfacial structure, hydrogen bonds and dynamics

Debashree Chakraborty[1,2], Bhabani S. Mallik[1,3] and Amalendu Chandra[1,*]

[1]Department of Chemistry, Indian Institute of Technology, Kanpur 208 016, India
[2]Present address: Institut de Biologie Physico-Chimique, Laboratoire de Biochimie Theorique, 13 Rue Pierre et Marie Curie, 75005 Paris, France
[3]Present address: Department of Chemistry, Indian Institute of Technology, Hyderabad 502 205, India

We present a theoretical study of the structure and dynamics of water–carbon tetrachloride liquid–liquid interface by means of *ab initio* molecular dynamics simulations. We have studied the density profiles, orientational profiles, hydrogen bond distributions, vibrational power spectra, diffusion, orientational relaxation, hydrogen bond dynamics and vibrational spectral diffusion of bulk and interfacial molecules. We have also provided an analysis of vacancies present in the interfacial system using Voronoi polyhedra method. The hydrogen bonding interaction is found to be weakened at the interface compared to that in the bulk phase of water. Weakly hydrogen bonded and non-hydrogen bonded water molecules at the interface give rise to peaks at different positions of the vibrational power spectrum. Diffusion and orientational relaxation of water molecules are also found to be faster at the interface, which can be correlated with the vacancies present in the system. The dynamics of vibrational spectral diffusion is studied by means of frequency–time correlations calculated through a time-series analysis using the wavelet method and the results of spectral diffusion are correlated with the dynamics of hydrogen bond fluctuations and that of non-hydrogen bonded hydroxyl modes in the bulk and interfacial regions.

Keywords: Carbon tetrachloride, hydrogen bonds, interfacial structure, molecular dynamics, water.

Introduction

THIS article deals with a detailed theoretical study of structural and dynamical properties of the liquid–liquid interface of water and carbon tetrachloride (CCl_4). Water is a unique solvent that plays a key role in a wide range of chemical, physical and biological processes[1–7]. Its uniqueness is due to its polarity and hydrogen bond properties which make it a universal solvent. Many theoretical and experimental studies have been carried out to develop a molecular picture of the structure and bonding of water at interfaces with other solids, liquids and gaseous systems. Studies of liquid–liquid interfaces of water with nonpolar hydrophobic solvents are of great importance in the fields of chemistry, biology, physics and environmental sciences. In the biological domain, membrane formation, protein folding, micelle formation and exchange of molecules across the cell membrane and many other processes involve interfaces where the interaction of water with a hydrophobic surface plays an important role. Water molecules in the presence of a nonpolar hydrophobic surface suffer loss of hydrogen bonding partners at the interface[8–12], hence their behaviour can be rather different from those in bulk water where each water molecule is strongly hydrogen bonded to others in its vicinity. Water–carbon tetrachloride system provides an interesting liquid–liquid interfacial system, where behaviour of water near a fluid hydrophobic surface can be studied. This system has been studied in the past through both experimental and theoretical means. On the experimental side, Richmond and coworkers[13–18] used sum frequency generation (SFG) method to look at the interfacial behaviour of water–carbon tetrachloride and also some of the other liquid–liquid interfacial systems. These interfacial systems have also been studied by others[19–25]. For water–CCl_4 interface, it was found that unlike water vapour system, the hydrogen bond strength of water molecules at the interface is weaker for water–CCl_4 system. Further studies involving Raman spectral analysis also revealed the weakening of the hydrogen bonds of water molecules at the water–CCl_4 interface[26].

On the theoretical side, molecular dynamics simulations for water–CCl_4 and related liquid–liquid systems have been carried out by several groups using classical potential models[18,27–38]. In particular, we note the work of Benjamin[29], where classical molecular dynamics simulations of water–carbon tetrachloride and also of water–1-2 dichloroethane and water–nitrobenzene were performed. It was found that at the interfacial region, the hydrogen

*For correspondence. (e-mail: amalen@iitk.ac.in)

bonded water molecules take more time to find a new hydrogen bonding partner due to lack of the adjacent non-hydrogen bonded water molecules and this led to a slower hydrogen bond dynamics at the interface. The polarizable potential models have also been used to calculate the orientational correlations and the potential of mean force of water dimer in bulk water and in carbon tetrachloride and also the electrostatic properties at the interfaces[33,34]. It was shown that the differences in these properties in bulk and interfacial phases mainly arise from changes in the hydrogen bonding structure of water molecules in the two regions. Apart from this, theoretical studies regarding the behaviour of the solute molecules at liquid–liquid interfaces have also been performed. These work include vibrational relaxation[30], solvation dynamics[31], transport mechanism of ions[35,37] and organic solutes[36] across interfaces. Structural analysis of liquid–liquid interfaces at the molecular level has also been done using the method of so called 'identification of the truly interfacial molecules' (ITIM)[39–41]. These authors looked at the width and orientational properties of water–carbon tetrachloride and other related systems. It was found that the water molecules located at the interface with an apolar phase experience a rather special local environment due to which the water molecules form hydrogen bonds with their neighbouring water molecules that are stronger than the water–water hydrogen bonds in the bulk liquid phase[40]. This is different from the experimental findings reported in the literature[16,26]. Monte-Carlo calculations have also been carried out for studying the hydrogen bonded structure in the vicinity of apolar surfaces such as water–carbon tetrachloride and water–dichloroethane interfaces[42]. Several molecular properties of the interfaces such as interaction energies, hydrogen bond statistics and angle distributions were calculated. Studies of the intermolecular interactions and stable configurations for the 1 : 1 molecular clusters of methanol–CCl_4 and water–CCl_4 have also been carried out using *ab initio* molecular dynamics calculations[43].

In the present work, we have carried out a detailed analysis of the structural and dynamical properties of water–carbon tetrachloride interface using the method of *ab initio* molecular dynamics[44,45]. Structural and dynamical properties are studied through calculations of various equilibrium and time-correlation functions, including an analysis of vacancies using the Voronoi polyhedra method and a time-series analysis using the wavelet method. A thorough analysis of this liquid–liquid interfacial system by *ab initio* molecular dynamics simulations without using any empirical potential is presented here. In the present method, the quantum many-body potentials and the forces are calculated on the fly-through quantum electronic structure calculations within density functional theory. We have looked at various structural properties like hydrogen bond distributions, orientational profiles, voids in the system, vibrational power spectrum and frequency distributions of water molecules in the bulk and interfacial regions. On the dynamical side, we have studied the diffusion, orientational relaxation, dynamics of hydrogen bonds and dangling hydroxyl modes and also the dynamics of vibrational frequency fluctuations. Again, these calculations are done for both bulk and interfacial molecules. Connections are made with the experimental results wherever available for the current interfacial system.

We have organized the rest of the article as follows. The simulation details are discussed in the next section. The results of the structural properties of the current system are then discussed followed by the vibrational spectral properties of bulk and interfacial water molecules. We then present various dynamical properties and finally summarize our conclusions.

Simulation details

We first carried out a classical molecular dynamics simulation using model potentials[46,47] to create the initial configuration of water and CCl_4 molecules at a temperature of 300 K. Our simulation system consists of a total of 121 molecules containing 401 atoms (102 water and 19 CCl_4 molecules). First we simulated the water and CCl_4 in two separate cubic boxes, each of length 14.5 Å, at their experimental bulk densities at room temperature. These cubic boxes were periodically replicated in all the three dimensions. After the bulk liquids were separately equilibrated for 1 ns, these two boxes were joined along the z-dimension and the resultant larger rectangular box hence formed was taken as the simulation box for the next phase of the simulation runs. The dimensions of the larger rectangular box were 14.5 Å along x and y directions and 29.0 Å along the z direction. The system was equilibrated for 2 ns by imposing periodic boundary conditions in all the three dimensions. The final configuration after the classical runs was taken as the initial configuration for the *ab initio* simulations. The *ab initio* molecular dynamics simulations have been carried out by employing the Car–Parrinello method[44] and the CPMD code[48]. The electronic structure of the extended simulation system was represented by the Kohn–Sham (KS) formulation[49] of density functional theory within a plane wave basis. The core electrons were treated via the Vanderbilt ultrasoft pseudopotentials[50] and the plane-wave expansion of the KS orbitals was truncated at a kinetic energy of 25 Ry. A fictitious mass of $\mu = 800$ au was assigned to the electronic degrees of freedom and the coupled equations of motion describing the system dynamics were integrated using a time step of 5 au. The mass of deuterium was assigned to all the hydrogen atoms. We have used the BLYP density functional in the present simulations[51]. We equilibrated the systems for 10 ps in canonical ensemble and thereafter, we continued our runs in microcanonical ensemble for another 25 ps for

the calculation of various equilibrium and dynamical properties. The average density of water as found for the homogeneous bulk region was close to 1 g cm^{-3} and that of CCl_4 was close to the desired value of 1.58 g cm^{-3}. The average simulation temperature was found to be around 305 K.

Structural properties

Density and orientational profiles and hydrogen bond distribution

The density profiles of an interfacial system describe the inhomogeneity of the interface and also help in locating the interfacial region and its thickness. We have calculated the density profiles of water and CCl_4 molecules across the interface by calculating the average number of water and carbon tetrachloride molecules in slabs of thickness $\Delta z = 0.14$ Å and the results are shown in Figure 1 *a*. In this figure, we have shown the variation of density with z, where the coordinate z is along the surface normal and the centre of the simulation system is located at $z = 0$. For a liquid–liquid interface, the interfacial region starts where the densities of both liquids start decreasing from their bulk values. For the present system, it is seen that two density profiles cross at around $z = 0$, which can be taken as the centre of the interfacial zone. It is found that while the density of both the liquids decreases toward the centre of the interface, this decrease is not as sharp as was found for liquid–vapour interfaces. In order to have an estimate of the width of the interfacial region, we have used an extension of the so-called 90–10 rule that is commonly applied to liquid–vapour interfaces. On either side, we consider the beginning of the interface as the location where the density of the liquid on that side decreases to 90% of its bulk value. According to this definition, the width of the water–CCl_4 interface is found to be 5.03 Å, which is higher than typical width of about 3–4 Å for aqueous liquid–vapour interface reported in earlier studies[52–59]. We also note in this context that the interfacial width has a contribution from capillary waves[60–66] which give rise to an additional component of the width due to thermal fluctuations in the position of the interface. Hence, the observed changes of the number densities at interfaces have contributions both from intrinsic changes of the density profiles and also from broadening due to capillary wave fluctuations as allowed by the length and timescales of the present simulations.

We have also calculated the molecular orientation of water molecules near the CCl_4 surface. The orientation of a water molecule is defined in terms of the angle θ that the molecular dipole vector makes with the surface normal along the z axis. In Figure 1 *b*, we have shown the angular distributions of water molecules in the bulk and interfacial regions. It can be seen that in the bulk phase, the probability distribution is almost uniform since there is no preferred orientation of water molecules in the homogeneous bulk phase. However, for the interfacial water molecules, a maximum is found at around $\cos\theta = 0$, which means that the molecules at the interface prefer to orient with their dipoles parallel to the surface. One H atom of water points towards the CCl_4 side and the other hydrogen points towards the aqueous phase. This can be related to the findings of Richmond and coworkers[67], who found that the parameter $S_1 < 0$ for water molecules at the interface, which means that the interface mainly consists of water molecules with one of their OH bonds projecting towards the bulk water phase and another pointing towards CCl_4 phase. Also, some of the water molecules at the interface are oriented such that the two OH bonds are in the plane of the interface. The hydrogen bond distribution of the water molecules is shown in Figure 1 *c*. It is calculated from the average number of hydrogen bonds per water molecule in the slabs of thickness $\Delta z = 0.14$ Å. We have used a geometric criterion where two water molecules are taken to be hydrogen bonded if their hydrogen–oxygen distance is less than 2.4 Å. Since the number of water molecules decreases on approaching the interface, the number of hydrogen bonds per water molecule is also found to decrease in the interfacial region.

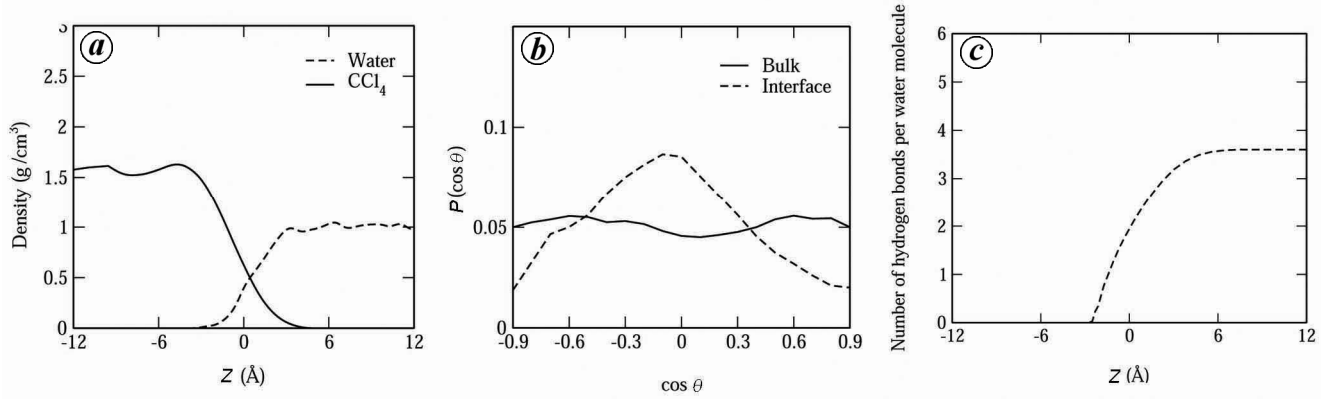

Figure 1. ***a***, Density profiles of water and carbon tetrachloride; ***b***, Orientation profiles of water; ***c***, Hydrogen bond distributions of water in bulk and interfacial regions.

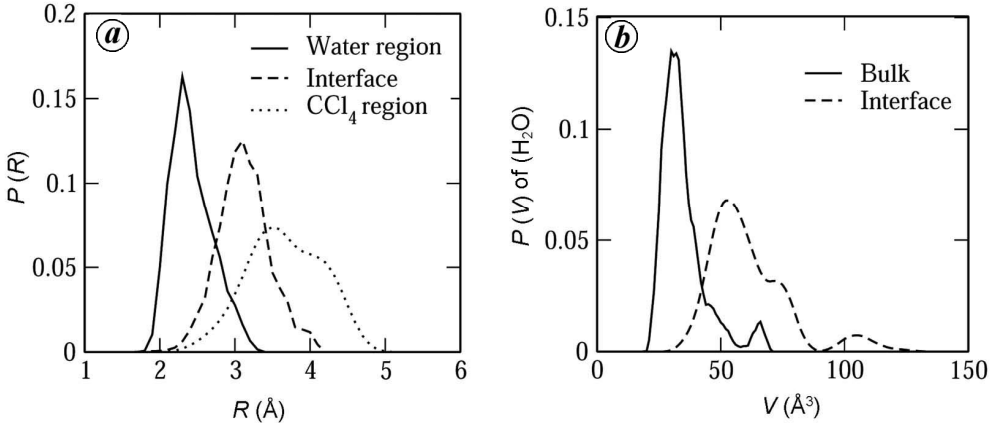

Figure 2. Probability distribution of (***a***) radius of vacancies and (***b***) volume of Voronoi polyhedra of water molecules in the bulk and interfacial regions.

Analysis of vacancies

Apart from density profiles, another way of characterizing the structural properties of a liquid system is by calculating the vacancies present in the system. The vacancies are calculated using the method of Voronoi polyhedra (VP) analysis[68], the details of which can be found in ref. 69. From a set of configuration of atoms, we can generate a tessellation in the three-dimensional space known as the Voronoi tessellation. This consists of repeated units of the Voronoi polyhedra regions of atoms. A Voronoi polyhedra region of an atom i, $\prod_i$, is defined as the region in which all points in the space are closer to that atom than to any other atom and the vacancy radius is defined as the distance between the Voronoi polyhedra vertex and the atom[70,71]. Another way of defining the void space is through Delaunay triangulation[72]. Voronoi polyhedra and Delaunay triangulation are complementary to each other. We have carried out the Voronoi and Delaunay tessellation analysis by using the algorithm given in refs 69, 73. We have calculated the radius of vacancies and the volume of VP along the z coordinate of the water–CCl_4 system to show how the radius of vacancies and the volume of VP change as we move from the bulk phases toward the interface. In carrying out the Voronoi analysis, we have considered the coordinates of only the heavy atoms. In Figure 2, we have shown the distributions of the radius of vacancies and the volume of VP of the bulk and interfacial water molecules. The most probable radius of vacancies in bulk water is found to be 2.3 Å and it is 3.2 Å at the interface. The most probable radius of vacancies in bulk CCl_4 phase is 3.75 Å. Since the number of water molecules decreases at the interfacial region, the vacancy radius and the volume of VP also increase. As CCl_4 has less number density, the size of the vacancies and VP in the bulk phase of this liquid is higher than that in bulk liquid water.

Vibrational frequencies

Time series analysis

The time-dependent vibrational frequencies of the OD bonds are calculated through a time-series analysis of the *ab initio* molecular dynamics trajectories using wavelet method[74]. Here we briefly outline the key points of the method, since the details are available elsewhere[74–78]. In this method, a time-dependent function $f(t)$ is expressed in terms of the basis functions which are constructed as the translations and dilations of the mother wavelet ψ. For the mother wavelet, we have used the Morlet–Grossman wavelet[79].

$$\psi(t) = \frac{1}{\sigma\sqrt{2\pi}} e^{2\pi i\lambda t} e^{-t^2/2\sigma^2}, \tag{1}$$

with $\lambda = 1$, $\sigma = 2$ and i represents the imaginary number. The mother wavelet is scaled by a factor of a and translated by a factor of b to give

$$\psi_{a,b}(t) = \frac{1}{\sqrt{a}} \psi\left(\frac{t-b}{a}\right). \tag{2}$$

The coefficients of the wavelet expansion of $f(t)$ are given by the wavelet transform of $f(t)$, which is defined as

$$L_\psi f(a,b) = \frac{1}{\sqrt{a}} \int_{-\infty}^{+\infty} f(t) \bar{\psi}\left(\frac{t-b}{a}\right), \tag{3}$$

for $a > 0$ and b real. Therefore, $L_\psi f(a, b)$ gives the frequency content of $f(t)$ over the time window about b. The inverse of the scale factor a is proportional to the frequency. Following our previous work[76–78], the time-dependent function $f(t)$ for an OD bond is constructed as

a complex function with the real and the imaginary parts corresponding to the instantaneous fluctuations in OD distance and the momentum along the OD vector at time t. The stretch frequency of this bond at time $t = b$ is then determined from the scale a that maximizes the modulus of the corresponding wavelet transform at b.

Vibrational power spectrum

Information about the effects of hydrogen bonds on the dynamical behaviour of bulk and interfacial water molecules can be obtained from the power spectral analysis of velocity autocorrelation function of water molecules. The power spectrum of the velocity correlation function is defined as the cosine transform as follows

$$S(\omega) = \int_0^\infty C(t) \cos \omega t \, dt, \tag{4}$$

where $C(t)$ represents the time correlation of atomic velocities. We have studied the power spectrum of the bulk and interfacial water molecules at the stretching regions. Figure 3 *a* presents the power spectrum of the O-D stretch modes of bulk and interfacial water molecules. The power spectrum of the bulk molecules mainly consists of a broad spectrum of the strongly hydrogen bonded water molecules, whereas the power spectrum of the interfacial molecules consists of a broad spectral region arising from hydrogen bonded OD modes and a sharp peak arising from the dangling OD modes at the interface. We have also calculated the population distribution of water molecules in different hydrogen bonding environments in the interfacial region. In Figure 3 *a* (inset), the population distribution at the interface is shown, where it can be seen that the population of water with a dangling OD bond is maximum. At the interface, the probability of finding single donor (SD)-type water molecule is maximum (about 52%) and the probability of finding a double donor (DD)-type water and a non-donor (ND)-type water is 39% and 9% respectively. In the bulk phase, the population of the DD-type water molecules increases to about 69% and that of SD-type water molecules decreases to 31%. From the calculations of power spectral analysis of water molecules in different hydrogen bonding environments, we could assign the different peaks of the spectrum of the interface to different types of water molecules present in the region. Since water molecules with two acceptors and two donors (AADD type) are the ones which are maximally hydrogen bonded, they show maximum red shift and the corresponding peak for OD stretch is found to be at about 2228 cm^{-1}. This is followed by the ADD molecules having one acceptor and two donor hydrogen bonds with their OD stretch peak appearing at 2330–2360 cm^{-1}. Next comes the spectrum of the AD molecules with one acceptor and one donor hydrogen bonds with their peaks for the bonded and dangling OD modes (of also AA/A types) located at around 2475 and 2580 cm^{-1} respectively. Therefore, as the hydrogen bond strength of water molecules decreases, the corresponding frequency of the OD modes increases. This calculated power spectrum of interfacial water molecules can be nicely correlated with experimental studies[16].

In Figure 3 *b*, we have shown the frequency distribution calculated from the wavelet analysis for the hydrogen bonded (through D) and free OD groups present in the bulk and interface. Here it is found that the frequencies of the interfacial molecules are somewhat higher than those of the bulk molecules. The frequencies of non-hydrogen bonded OD modes of interfacial molecules are most blue-shifted, whereas hydrogen bonded OD modes in the bulk phase are maximally red-shifted. These results are in accordance with those of our power spectrum calculations shown in Figure 3 *a*. In Figure 4, we have

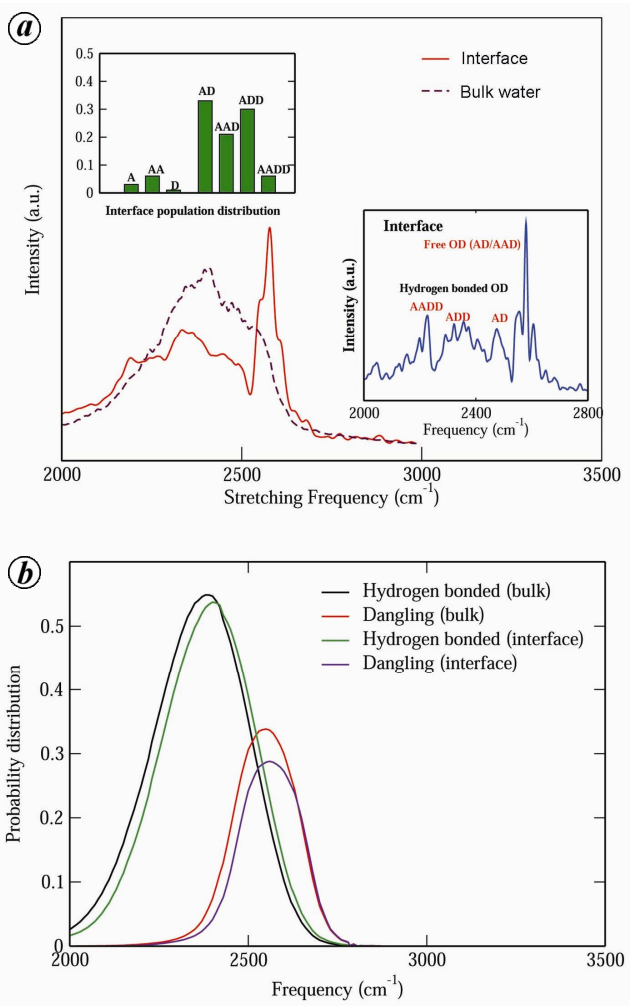

Figure 3. Power spectrum (***a***) and Probability distribution (***b***) of OD stretch frequencies of water molecules in bulk and interfacial regions. (Insets) Population distribution of interfacial water in different hydrogen bonding states and the assignment of peaks at different frequencies to OD modes of water in different hydrogen bonding states.

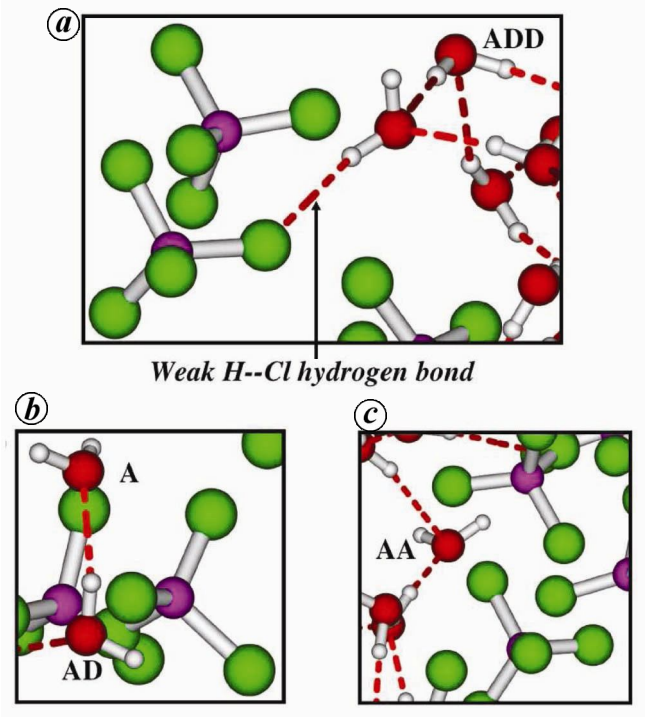

Figure 4. Snapshots taken from the simulation trajectory showing water in different hydrogen bonding states at the interface. Details are given in the text.

shown snapshots of water molecules in different hydrogen bonding environments in the interfacial region.

Dynamical properties

Diffusion

In the present water–carbon tetrachloride system, water molecules can move between interfacial and bulk phases, hence the probability of an interfacial molecule to remain continuously at the interface is not unity. The diffusion coefficient of water molecules in such an interface is calculated using the method of Liu *et al.*[80] which involves calculations of the mean square displacement and survival probability of a molecule in the interfacial region. We define $P_c(t)$ as the continuous survival probability of a molecule to remain continuously in the interfacial region over the time interval from $t = 0$ to t and $\langle \Delta x(t)^2 \rangle_i$ as the mean square displacement along the x-direction of the particles that remain in the interfacial region over the time interval $t = 0$ to t. The long time limit of the interfacial mean square displacement (MSD) is given by[80]

$$\langle \Delta x(t)^2 \rangle_i = 2P_c(t)D_x(I)t. \tag{5}$$

Hence the parallel diffusion coefficient of the interfacial molecules along the x and y-directions will be given by

$$D_{x,y}(I) = \lim_{t\to\infty} \frac{\langle \Delta x(t)^2 \rangle_i + \langle \Delta y(t)^2 \rangle_i}{4tP_c(t)}. \tag{6}$$

In Figure 5, we have shown the time dependence of MSD of the bulk and interfacial water molecules. For the interface, we have shown the time dependence of MSD of interfacial molecules divided by the corresponding survival probability. The diffusion coefficients of water as obtained from the long time slopes of the results shown in Figure 5 are found to be 0.46×10^{-5} cm^2 s^{-1} and 1.97×10^{-5} cm^2 s^{-1} for bulk and interfacial regions respectively. The diffusion coefficient of CCl_4 is 0.13×10^{-5} cm^2 s^{-1} for bulk and 0.27×10^{-5} cm^2 s^{-1} for the interface. Clearly, the interfacial molecules are more diffusive than the bulk molecules, which can be attributed to the reduced number density, less number of hydrogen bonds and weaker intermolecular interactions in the interfacial region.

Orientational relaxation

The rotational dynamics of water molecules is an important dynamical property since it is known to play a primary role in the breaking and reformation of hydrogen bonds. It is calculated from the orientational relaxation of the dipole vector of water molecules. The orientational time correlation function $C_l(t)$ is given by

$$C_l(t) = \frac{\langle P_l(\hat{e}(0)\cdot\hat{e}(t))\rangle}{\langle P_l(\hat{e}(0)\cdot\hat{e}(0))\rangle}, \tag{7}$$

where P_l is the Legendre polynomial of rank l and $\hat{e}(t)$ denotes the unit vector along the dipole vector. The experimentally measured rotational anisotropy is directly related to the second-rank rotational function $C_2(t)$. We have estimated the reorientational relaxation of the molecular dipole $C_2^{\mu}(t)$ vectors for the bulk and interfacial regions. The time dependence of the second-rank orientational correlation function of dipole vectors of the bulk and interfacial molecules is shown in Figure 6. The second-rank orientational time for the bulk and interface as obtained by integrating $C_2^{\mu}(t)$ is 4.38 and 3.89 ps respectively. As evident from this figure, there is a fast inertial decay followed by a slower diffusional relaxation. The weight of the inertial decay component is found to be higher for the interfacial molecules as these molecules can rotate more freely due to lower density and reduced number of hydrogen bonds.

Dynamics of hydrogen bonds

The main objective of this section is to study the hydrogen bond dynamics of water molecules in the vicinity of CCl_4 surface. We have calculated the hydrogen bond dynamics of the system using the population correlation

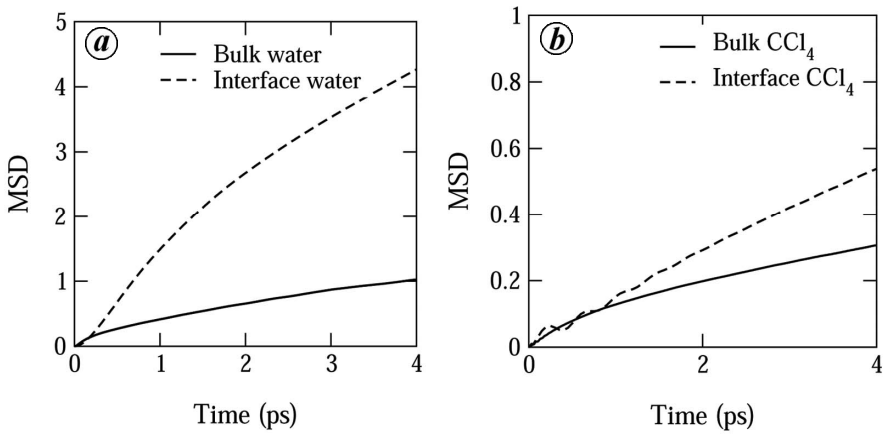

Figure 5. Time dependence of the mean square displacement of bulk and interfacial (***a***) water and (***b***) CCl_4 molecules. For the interfacial molecules, the mean square displacement is divided by the continuous survival probability.

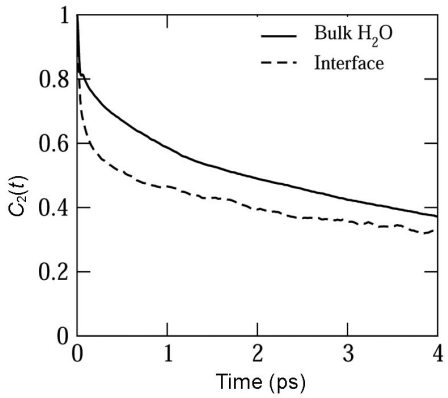

Figure 6. Time dependence of the second-rank dipole orientational correlation functions of water molecules in the bulk and interfacial regions.

Table 1. Values of the average lifetimes of hydrogen bonds (τ_{HB}) and dangling OD modes (τ_{DH})

Region	τ_{HB} (ps)	τ_{DH} (ps)
Bulk	2.25	0.20
Interface	1.80	1.85

function approach. Following previous work[81–87], we define a continuous hydrogen bond population variable, $H(t)$, which is unity if two molecules remain continuously hydrogen bonded from time $t = 0$ to $t = t$, and it is zero otherwise. The continuous correlation function $S_{HB}(t)$ is then defined as $S_{HB} = \langle H(0)H(t)\rangle/\langle H(0)^2\rangle$, where $\langle\ldots\rangle$ denotes an average over all water pairs in a given region. So, it gives the probability that an initially hydrogen bonded water pair in a given region remains bonded at all times up to t. The associated integrated relaxation time τ_{HB} gives the average hydrogen bond lifetime. We have used a set of geometric criteria to define the hydrogen bonds between two water molecules as described in the previous section. The results of S_{HB} for the bulk and interfacial water molecules are shown in Figure 7. The lifetimes of hydrogen bonds, as obtained by integration of $S_{HB}(t)$, are found to be 2.25 and 1.8 ps respectively, for bulk and interfacial regions. The bulk hydrogen bond lifetime agrees well with our previous *ab initio* molecular dynamics simulations of bulk water[76].

We have also calculated the continuous correlation function of dangling OD modes, $S_{DH}(t)$, which gives the probability that an initially non-hydrogen-bonded OD group remains dangling at all times from $t = 0$ to time t. In Figure 7, we have shown the time dependence of $S_{DH}(t)$ of the bulk and interfacial water molecules. The average lifetimes of OD bonds of the bulk and the interfacial water molecules to remain continuously dangling, which we refer to as the dangling lifetimes, are 0.19 and 1.85 ps respectively. In bulk water, the breaking and making of hydrogen bonds take place more frequently. Hence the lifetime of a dangling OD mode is very small. However, less number of water molecules is present at the interface and hence there is less cooperativity among molecules leading to a reduced scope of forming new hydrogen bonds unlike bulk water. This lack of cooperativity leads to a situation where a dangling OD mode remains dangling for a longer time. The values of the hydrogen bond and dangling OD time scales are shown in Table 1.

Time correlation of frequency fluctuations

The stretching frequencies of water molecules are highly sensitive to their local environments. Hence the dynamics of frequency fluctuations of OD stretch modes can be used to gain insights into environmental fluctuations, particularly those in the hydrogen bonds. The time dependence of vibrational frequency fluctuations is called vibrational spectral diffusion and it can be studied through calculations

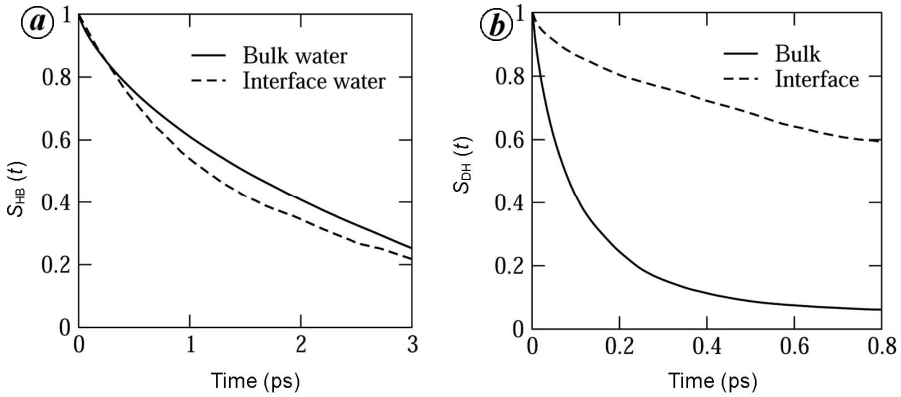

Figure 7. Time dependence of (***a***) continuous hydrogen bond correlation function $S_{HB}(t)$ and (***b***) continuous dangling correlation function $S_{DH}(t)$ of the bulk and interfacial water molecules.

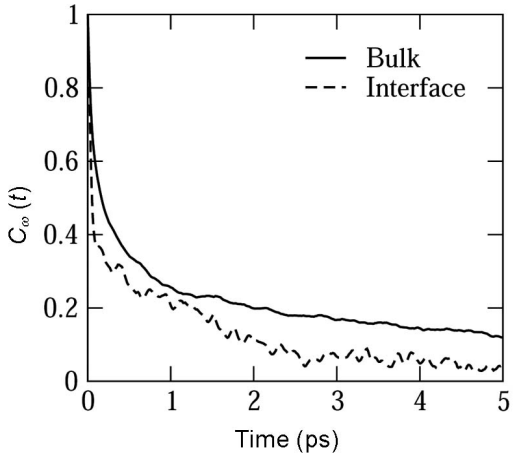

Figure 8. Time correlation function of fluctuating frequencies of OD modes of water molecules in the bulk and interfacial regions.

Table 2. Relaxation times (with corresponding weights) of frequency correlations of the OD stretch modes of bulk and interfacial water. The averages were carried out over those OD modes which were dangling at the initial time

Region	τ_1 (ps)	τ_2 (ps)	a_1	a_2
Bulk	0.22	2.6	0.45	0.55
Interface	0.08	1.95	0.46	0.54

of time correlation of fluctuating frequencies. We, therefore, have looked at the frequency fluctuations of the vibrational stretch frequencies of water molecules present in the bulk and also at the interfacial regions. The frequency time correlation function is defined as

$$C_\omega(t) = \frac{\langle \delta\omega(t)\delta\omega(0)\rangle}{\delta\omega(0)^2}, \quad (8)$$

where $\delta\omega(t)$ is the fluctuation from the average frequency at time t. The average of this equation is over the initial time and over all the OD groups of interest. We have calculated the frequency correlations for those OD bonds which were dangling at the initial time ($t = 0$). The results of the frequency time-correlation functions are shown in Figure 8 for both bulk and interfacial molecules. These correlations show a fast decay at short times followed by a slower decay extending up to few picoseconds. These functions are fitted by biexponential functions and the resultant weights and relaxation times are included in Table 2.

Studies of vibrational spectral diffusion in bulk water have attributed the short time decay component to fast modulation of stretch frequencies of OD modes of an intact hydrogen bonded pair[76,88–96]. As water molecules at the interface can move more freely, the weight of this fast component is seen to be higher for interfacial molecules. The slower long time decay can be attributed to breaking dynamics of hydrogen bonds. Hydrogen bond reformation dynamics, which also occurs with a slower timescale for interfacial phase as revealed from the lifetimes of dangling OD modes, can also contribute to this slower long time dynamics of the vibrational frequency fluctuations of interfacial molecules.

It is seen from the present calculations that the average lifetime of interfacial water–water hydrogen bonds is slightly shorter than that of bulk water. Earlier simulation studies of similar systems using classical models reported a slower hydrogen bond dynamics for interfacial molecules[97–103]. Since the interface is characterized by reduced density of water, there are reduced cooperative effects among water molecules at the interface which can lead to a slower dynamics of hydrogen bond breaking and reformation. Indeed, this was the case for liquid–vapour interfaces[59] and was also cited as a possible reason for slower hydrogen bond dynamics found in classical model-based studies in earlier simulations of liquid–liquid interfaces[29]. The present *ab initio* simulations revealed that a weak hydrogen bonding interaction exists between hydrogen atoms of water and chlorine atom of CCl_4 at the interface (Figure 4). This can be seen from

Figure 9 which shows the distribution of H···Cl distance between a water hydrogen and its nearest chlorine of CCl_4 at the interface. It is clear that there is a significant probability of finding an H···Cl pair within a distance of about 3.0 Å, which is the typical cut-off distance of a hydrogen bond between a hydrogen atom of water and a charged chlorine atom[104]. The reason for this weak hydrogen bonding interaction between water and CCl_4 can be attributed to partial charges on chlorine atoms arising from higher electronegativity of chlorine and also to its high polarizability. Both these effects are automatically incorporated in the present quantum chemical calculations of interactions and forces, hence such weak hydrogen bonding effects are seen in the present study. The binding energy of H_2O–CCl_4 dimer was earlier calculated to be 1.4 kcal/mol (ref. 16). It has been found from the orientational profiles that a water molecule at the interface prefers to orient in a manner such that one of its OD bonds is directed towards the bulk phase and other one towards CCl_4. This orientational preference also favours a weak hydrogen bonding interaction between water and CCl_4 molecules at the interface. These weak H···Cl hydrogen bonds provide a second channel of cooperativity in addition to water–water hydrogen bonds and can favour hydrogen bond breaking and reformation events. This could be a possible reason, in addition to other effects such as enhanced diffusion and orientational relaxation, for our finding a slightly shorter lifetime of interfacial hydrogen bonds compared to that in the bulk phase of water.

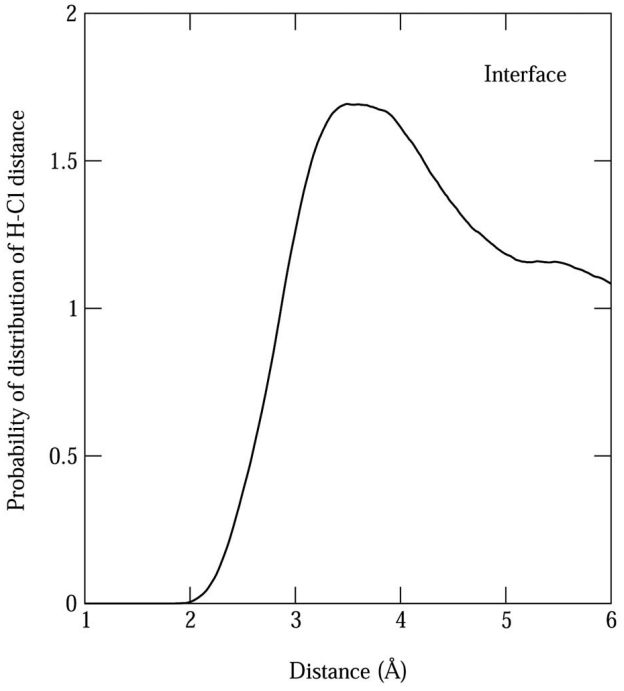

Figure 9. Probability distribution of the distance of D (of water) and its nearest Cl (of CCl_4) at the interface.

Conclusions

We have presented a first principles theoretical study of the structure and dynamics of the liquid–liquid interface of water–carbon tetrachloride system. We have generated the trajectories by carrying out *ab initio* molecular dynamics simulations using the Car–Parrinello technique[44] and various properties are calculated by employing a combination of equilibrium and dynamical methods. Among the structural properties, we have calculated the density profiles, orientational profiles, hydrogen bond distributions, vibrational power spectrum, frequency distributions and also the voids present in the system in bulk and interfacial regions. As the interface is approached, the density of water molecules and the number of hydrogen bonds per water molecule decrease. Due to this decreased density, the radius of voids and the volume available to the particles increase at the interface. It is found that the water molecules at the interface are preferentially oriented with one OD of each water pointing towards the bulk phase and the other pointing towards the CCl_4 side. The calculated vibrational power spectrum of the interfacial water molecules agrees well with the experimental findings of ref. 16. The distributions of OD stretching frequencies are also calculated through a time series analysis and the results are obtained for different hydrogen bonding environments in the bulk and interfacial regions. The current study also reveals the presence of a weaker hydrogen bonding interaction between water and CCl_4 molecules in the interfacial region.

On the dynamical side, the interfacial molecules are found to be more diffusive than the bulk molecules. This happens due to reduced density and less number of hydrogen bonds at the interface. These effects also lead to an increased weight of the fast inertial component of the rotational relaxation of interfacial molecules. We have calculated the hydrogen bond dynamics of this system using population correlation method and have correlated the dynamics with the results of vibrational frequency fluctuations calculated through time correlations of fluctuating frequencies of bulk and interfacial water molecules. The longer timescales of the frequency–time correlations are found to agree well with the lifetimes of hydrogen bonds. The present study reveals a slightly shorter lifetime of interfacial hydrogen bonds compared to that in bulk water. We note that this behaviour is different from the predictions of earlier studies which used classical potential models[29]. This slight acceleration of hydrogen bond dynamics at the interface is attributed to faster rotational and translational motion of interfacial molecules and also to the formation of weak H···Cl hydrogen bonds between water and CCl_4 at the interface. The possibility of formation of such weak hydrogen bonds, in addition to water–water hydrogen bonds, adds to the cooperativity among interfacial molecules and thus favours hydrogen bond breaking and reformation events.

We finally note that a dispersion corrected version of the BLYP functional, the so-called BLYP-D functional or its variants[105], has been used in some of the recent studies of aqueous systems as inclusion of such dispersion corrections has been shown to produce an improved phase diagram of water[106,107]. In the present work, no such additional dispersion correction has been included in the *ab initio* simulations. However, simulations of the water–carbon tetrachloride interface with a dispersion-corrected density functional is currently in progress and the results of such calculations will be reported in a future publication.

1. Eisenberg, D. and Kauzmann, W., *The Structure and Properties of Water*, Oxford University Press, New York, 1969.
2. Franks, F., *Water – A Comprehensive Treatise*, Plenum, New York, 1972.
3. Clark, G. N. I., Cappa, C. D., Smith, J. D., Saykally, R. J. and Head-Gordon, T., The structure of ambient water. *Mol. Phys.*, 2010, **108**, 1415–1433.
4. Nandi, N., Bhattacharyya, K. and Bagchi, B., Dielectric relaxation and solvation dynamics of water in complex chemical and biological systems. *Chem. Rev.*, 2000, **100**, 2013–2045; Bagchi, B., Water dynamics in the hydration layer around proteins and micelles. *Chem. Rev.*, 2005, **105**, 3197–3219.
5. Moreno, M., Frutos, P. and Ballesteros, M. P., Lyophilized lecithin based oil–water microemulsions as a new and low toxic delivery system for amphotericin B. *Pharm. Res.*, 2001, **18**, 344–351.
6. Dickinson, E., Euston, S. R. and Woskett, C. M., Competitive adsorption of food macromolecules and surfactants at the oil–water interface. *Prog. Colloid Polym. Sci.*, 1990, **82**, 65–75.
7. Handa, T., Saito, H. and Miyajima, K., Phospholipid monolayers at the trioleinsaline interface: production of microemulsion particles and conversion of monolayers to bilayers. *Biochemistry*, 1990, **29**, 2884–2890.
8. Stillinger, F. H., Structure in aqueous solutions of nonpolar solutes from the standpoint of scaled-particle theory. *Solut. Chem.*, 1973, **2**, 141–158.
9. Lee, C., McCammon, J. and Rossky, P., The structure of liquid water at an extended hydrophobic surface. *J. Chem. Phys.*, 1984, **80**, 4448–4455.
10. Lum, K., Chandler, D. and Weeks, J. D., Hydrophobicity at small and large length scales. *J. Phys. Chem. B*, 1999, **103**, 4570–4577.
11. Choudhury, N. and Pettitt, B. M., On the mechanism of hydrophobic association of nanoscopic solutes. *J. Am. Chem. Soc.*, 2005, **127**, 3556; Enthalpy–entropy contributions to the potential of mean force of nanoscopic hydrophobic solutes. *J. Phys. Chem. B*, 2006, **110**, 8459–8463.
12. Rana, M. and Chandra, A., *Ab initio* and classical molecular dynamics studies of the structural and dynamical behavior of water near a hydrophobic graphene sheet. *J. Chem. Phys.*, 2013, **138**, 204702; Solvation structure of nanoscopic hydrophobic solutes in supercritical water: Results for varying thickness of hydrophobic walls, solute–solvent interaction and solvent density. *Chem. Phys.*, 2012, **408**, 28–35.
13. Richmond, G. L., Molecular bonding and interactions at aqueous surfaces as probed by vibrational sum frequency spectroscopy. *Chem. Rev.*, 2002, **102**, 2693–2724.
14. Conboy, J. C., Messmer, M. C., Walker, R. A. and Richmond, G. L., An investigation of surfactant behavior at the liquid/liquid interface with sumfrequency vibrational spectroscopy. *Prog. Colloid Polym. Sci.*, 1997, **103**, 10–20.
15. Scatena, L. F. and Richmond, G. L., Orientation, hydrogen bonding, and penetration of water at the organic/water interface. *J. Phys. Chem. B*, 2001, **105**, 11240–11250.
16. Scatena, L. F., Brown, M. G. and Richmond, G. L., Water at hydrophobic surfaces: weak hydrogen bonding and strong orientation effects. *Science*, 2001, **292**, 908–911.
17. Richmond, G. L., Structure and bonding of molecules at aqueous Surfaces. *Annu. Rev. Phys. Chem.*, 2001, **52**, 357–389.
18. Moore, F. G. and Richmond, G. L., Integration or segregation: how do molecules behave at oil/water interfaces? *Acc. Chem. Res.*, 2008, **41**, 739–748.
19. Higgins, D. A. and Corn, R. M., Second harmonic generation studies of adsorption at a liquid–liquid electrochemical interface. *J. Phys. Chem.*, 1993, **97**, 489–493.
20. Grubb, S. G., Kim, M. W., Rasing, T. and Shen, Y. R., Orientation of molecular monolayers at the liquid–liquid interface as studied by optical second harmonic generation. *Langmuir*, 1988, **4**, 452–454.
21. Conboy, J. C., Daschbach, J. L. and Richmond, G. L., Studies of alkane/water interfaces by total internal reflection second harmonic generation. *J. Chem. Phys.*, 1994, **98**, 9688–9692.
22. Du, Q., Superfine, R., Freysz, E. and Shen, Y. R., Vibrational spectroscopy of water at the vapor/water interface. *Phys. Rev. Lett.*, 1993, **70**, 2313–2316.
23. Eisenthal, K. B., Equilibrium and dynamic processes at interfaces by second harmonic and sum frequency generation. *Annu. Rev. Phys. Chem.*, 1992, **43**, 627–661.
24. Eisenthal, K. B., Liquid interfaces probed by second-harmonic and sum-frequency spectroscopy. *Chem. Rev.*, 1996, **96**, 1343–1360.
25. Tian, C. S. and Shen, Y. R., Structure and charging of hydrophobic material/water interfaces studied by phase-sensitive sum-frequency vibrational spectroscopy. *Proc. Natl. Acad. Sci.*, 2009, **106**, 15148–15153.
26. Serio, M. D., Mohapatra, H., Zenobi, R. and Deckert, V., Investigation of the liquid–liquid interface with high spatial resolution using near-field Raman spectroscopy. *Chem. Phys. Lett.*, 2006, **417**, 452–456.
27. Walker, D. S. and Richmond, G. L., Depth profiling of water molecules at the liquid–liquid interface using a combined surface vibrational spectroscopy and molecular dynamics approach. *J. Am. Chem. Soc.*, 2007, **129**, 9446–9451.
28. Benjamin, I., Molecular structure and dynamics at liquid–liquid interfaces. *Annu. Rev. Phys. Chem.*, 1997, **48**, 407–451.
29. Benjamin, I., Hydrogen bond dynamics at water/organic liquid interfaces. *J. Phys. Chem. B*, 2005, **109**, 13711–13715.
30. Benjamin, I., Vibrational relaxation at the liquid/liquid interface. *J. Chem. Phys.*, 2004, **121**, 10223–10232.
31. Michael, D. and Benjamin, I., Molecular dynamics computer simulations of solvation dynamics at liquid/liquid interfaces. *J. Chem. Phys.*, 2001, **114**, 2817–2824.
32. Moreira, N. H. and Skaf, M. S., Structural characterization of the H_2O/CCl_4 liquid interface using molecular dynamics simulations. *Prog. Colloid Polym. Sci.*, 2004, **128**, 81–85.
33. Chang, T. M. and Dang, L. X., Molecular dynamics simulations of CCl_4–H_2O liquid–liquid interface with polarizable potential models. *J. Chem. Phys.*, 1995, **104**, 6772–6783.
34. Chang, T. M. and Dang, L. X., Computational studies of liquid water and diluted water in carbon tetrachloride. *J. Phys. Chem. A*, 2008, **112**, 1694–1700.
35. Wick, C. D. and Dang, L. X., Distribution, structure, and dynamics of cesium and iodide Ions at the H_2O–CCl_4 and H_2O-vapor interfaces. *J. Phys. Chem. B*, 2006, **110**, 6824–6831.
36. Chang, T. M. and Dang, L. X., Transfer of CH_4 across the H_2O–CCl_4 liquid–liquid interface with polarizable potential models. *Chem. Phys. Lett.*, 1996, **263**, 39–45.
37. Dang, L. X., Computer simulation studies of ion transport across a liquid/liquid interface. *J. Phys. Chem. B*, 1999, **103**, 8195–8200.
38. Ishiyama, T., Sato, Y. and Morita, A., Interfacial structures and vibrational spectra at liquid/liquid boundaries: molecular dynam-

ics study of water/carbon tetrachloride and water/1,2-dichloroethane interfaces. *J. Phys. Chem. C*, 2012, **116**, 21439–21446.
39. Jedlovszky, P., Vincze, A. and Horvai, G., Full description of the orientational statistics of molecules near to interfaces. Water at the interface with CCl_4. *Phys. Chem. Chem. Phys.*, 2004, **6**, 1874–1879.
40. Partay, L. B., Horvai, G. and Jedlovszky, P., Molecular level structure of the liquid/liquid interface. Molecular dynamics simulation and ITIM analysis of the water–CCl_4 system. *Phys. Chem. Chem. Phys.*, 2008, **10**, 4754–4764.
41. Hantal, G., Darvas, M., Partay, L. B. and Jedlovszky, P., Molecular level properties of the free water surface and different organic liquid/water interfaces, as seen from ITIM analysis of computer simulation results. *J. Phys. Condens. Matter*, 2010, **22**, 284112.
42. Jedlovszky, P., The hydrogen bonding structure of water at the vicinity of apolar interfaces: A computer simulation study. *J. Phys. Condens. Matter*, 2004, **16**, S5389–S5402.
43. Torii, H., Atomic quadrupolar effect in the methanol–CCl_4 and water–CCl_4 intermolecular interactions. *Chem. Phys. Lett.*, 2004, **393**, 153–158.
44. Car, R. and Parrinello, M., Unified approach for molecular dynamics and density-functional theory. *Phys. Rev. Lett.*, 1985, **55**, 2471–2474.
45. Marx, D. and Hutter, J., *Ab initio Molecular Dynamics: Basic Theory and Advanced Methods*, Cambridge University Press, Cambridge, 2009.
46. Berendsen, H. J. C., Grigera, J. R. and Straatsma, T. P., The missing term in effective pair potentials. *J. Phys. Chem.*, 1987, **91**, 6269–6271.
47. McDonald, R., Bounds, D. G. and Klein, M. L., Molecular dynamics calculations for the liquid and cubic plastic crystal phases of carbon tetrachloride. *Mol. Phys.*, 1982, **45**, 521.
48. Hutter, J. *et al.*, CPMD Program, MPI für Festkörperschung, Stuttgart 1997–2001 and IBM Corp. 1990–2013, see www.cpmd.org
49. Kohn, W. and Sham, L. J., Self-consistent equations including exchange and correlation effects. *Phys. Rev. A*, 1965, **140**, 1133–1138.
50. Vanderbilt, D., Soft self-consistent pseudopotentials in a generalized eigenvalue formalism. *Phys. Rev. B*, 1990, **41**, 7892–7895.
51. Becke, A. D., Density-functional exchange-energy approximation with correct asymptotic behavior. *Phys. Rev. A*, 1988, **38**, 3098–3100; Lee, C., Yang, W. and Parr, R. G., Development of the Colle–Salvetti correlation-energy formula into a functional of the electron density. *Phys. Rev. B*, 1988, **37**, 785–789.
52. Stillinger, F. H. and Naim, A. B., Liquid–vapor interface potential for water. *J. Chem. Phys.*, 1967, **47**, 4431–4437.
53. Townsend, R. M., Gryko, J. and Rice, S. A., Structure of the liquid–vapor interface of water. *J. Chem. Phys.*, 1985, **82**, 4391–4392; Townsend, R. M. and Rice, S. A., Molecular dynamics studies of the liquid–vapor interface of water. *J. Chem. Phys.*, 1991, **94**, 2207–2218.
54. Wilson, M. A., Pohorille, A. and Pratt, L. R., Molecular dynamics of the water liquid–vapor interface. *J. Phys. Chem.*, 1987, **91**, 4873–4878; Wilson, M. A., Pohorille, A. and Pratt, L. R., Surface potential of the water liquid–vapor interface. *J. Chem. Phys.*, 1988, **88**, 3281.
55. Matsumoto, M. and Kataoka, Y., Study on liquid–vapor interface of water. I. Simulational results of thermodynamic properties and orientational structure. *J. Chem. Phys.*, 1988, **88**, 3233–3245.
56. Motakabbir, K. A. and Berkowitz, M. L., Liquid–vapor interface of TIP4P water: comparison between a polarizable and a nonpolarizable model. *Chem. Phys. Lett.*, 1991, **176**, 61–66.
57. Dang, L. X. and Chang, T. M., Molecular dynamics study of water clusters, liquid, and liquid–vapor interface of water with many-body potentials. *J. Chem. Phys.*, 1997, **106**, 8149–8159.
58. Benjamin, I., Vibrational spectrum of water at the liquid/vapor interface. *Phys. Rev. Lett.*, 1994, **73**, 2083–2086.
59. Paul, S. and Chandra, A., Hydrogen bond dynamics at vapour–water and metal water interfaces. *Chem. Phys. Lett.*, 2004, **386**, 218–224.
60. Steel, W. H. and Walker, R. A., Measuring dipolar width across liquid/liquid interfaces using molecular rulers. *Nature*, 2003, **424**, 296–298.
61. Mitrinovic, D. M., Zhang, Z., Williams, S., Huang, Z. and Schlossman, M. L., X-ray reflectivity study of the water–hexane interface. *J. Phys. Chem. B*, 1999, **103**, 1779–1782.
62. Mitrinovic, D. M., Tikhonov, A. M., Li, M., Huang, Z. and Schlossman, M. L., Non-capillary-wave structure at the water–alkane interface. *Phys. Rev. Lett.*, 2000, **85**, 582–585.
63. Bowers, J., Zarbakhsh, A., Webster, J. R. P., Hutcandhings, L. and Richards, R. W., Neutron reflectivity studies at liquid–liquid interfaces: methodology and analysis. *Langmuir*, 2001, **17**, 140–145.
64. Senapati, S. and Berkowitz, M. L., Computer simulation study of the interface width of the liquid/liquid interface. *Phys. Rev. Lett.*, 2001, **87**, 176101–176104.
65. Lacasse, M.-D., Grest, G. S. and Levine, A. J., Capillary-wave and chain-length effects at polymer/polymer interfaces. *Phys. Rev. Lett.*, 1998, **80**, 309–312.
66. Werner, A., Schmid, F., Müller, M. and Binder, K., Intrinsic profiles and capillary waves at homopolymer interfaces: A Monte Carlo study. *Phys. Rev. E*, 1999, **59**, 728–738.
67. Hore, D. K., Walker, D. S. and Richmond, G. L., Water at hydrophobic surfaces: when weaker is better. *J. Am. Chem. Soc.*, 2008, **130**, 1800–1801.
68. Voronoi, G., Nouvelles application des parametres continus a la theorie des formes quadratiques. *J. Reine Angew. Math.*, 1908, **134**, 199–287.
69. Tanemura, M., Ogawa, T. and Ogita, N., A new algorithm for three-dimensional Voronoi tessellation. *J. Comput. Phys.*, 1983, **51**, 191–207.
70. Yashonath, S. and Santikary, P., Diffusion in zeolites: Anomalous dependence on sorbate diameter. *J. Chem. Phys.*, 1994, **100**, 4013–4016; Yashonath, S. and Santikary, P., Diffusion of sorbates in zeolites Y and A: novel dependence on Sorbate size and strength of Sorbate–Zeolite interaction. *J. Phys. Chem.*, 1994, **98**, 6368–6376.
71. Ghorai, P. K. and Yashonath, S., The Stokes–Einstein relationship and the levitation effect: size-dependent diffusion maximum in dense fluids and close-packed disordered solids. *J. Phys. Chem. B*, 2005, **109**, 5824–5835.
72. Delaunay, B. N., 'Sur la sphere vide' Izvestia Akademia Nauk SSSR, 1934, vol. 7, p. 793.
73. Corti, D. S., Debenedetti, P. G., Sastry, S. and Stillinger, F. H., Constraints, metastability, and inherent structures in liquids. *Phys. Rev. E*, 1997, **55**, 5522–5534.
74. Vela-Arevalo, L. V. and Wiggins, S., Time-frequency analysis of classical trajectories of polyatomic molecules. *Int. J. Bifur. Chaos*, 2001, **11**, 1359–1380.
75. Semparithi, A. and Keshavamurthy, S., Intramolecular vibrational energy redistribution in DCO ($\tilde{X}^2\acute{A}$): Classical-quantum correspondence, dynamical assignments of highly excited states, and phase space transport. *Phys. Chem. Chem. Phys.*, 2003, **5**, 5051–5062.
76. Mallik, B. S., Semparithi, A. and Chandra, A., Vibrational spectral diffusion and hydrogen bond dynamics in heavy water from first principles. *J. Phys. Chem. A*, 2008, **112**, 5104–5112.
77. Mallik, B. S. and Chandra, A., Vibrational spectral diffusion in supercritical D_2O from the first principles: An interplay between the dynamics of hydrogen bonds, dangling OD groups and inertial rotation. *J. Phys. Chem. A*, 2008, **112**, 13518–13527.
78. Mallik, B. S., Semparithi, A. and Chandra, A., A first principle theoretical study of vibrational spectral diffusion and hydrogen bond dynamics in aqueous ionic solution: D_2O in hydration shells of Cl^- ions. *J. Chem. Phys.*, 2008, **129**, 194512-1–15.

79. Carmona, R., Hwang, W. and Torresani, B., *Practical Time–Frequency Analysis: Gabor and Wavelet Transforms with an Implementations in S*, Academic Press, New York, 1998.
80. Liu, P., Harder, E. and Berne, B. J., On the calculation of diffusion coefficients in confined fluids and interfaces with an application to the liquid–vapor interface of water. *J. Phys. Chem. B*, 2004, **108**, 6595–6602.
81. Rapaport, D. C., Hydrogen bonds in water. Network organization and lifetimes. *Mol. Phys.*, 1983, **50**, 1151.
82. Chandra, A., Effects of ion atmosphere on hydrogen-bond dynamics in aqueous electrolyte solutions. *Phys. Rev. Lett.*, 2000, **85**, 768–771; Chandra, A., Dynamical behavior of anion–water and water–water hydrogen bonds in aqueous electrolyte solutions: a molecular dynamics study. *J. Phys. Chem. B*, 2003, **107**, 3899–3906.
83. Chowdhuri, S. and Chandra, A., Hydrogen bonds in aqueous electrolyte solutions: Statistics and dynamics based on both geometric and energetic criteria. *Phys. Rev. E*, 2002, **66**, 041203-1-7.
84. Balasubramanian, S., Pal, S. and Bagchi, B., Hydrogen–bond dynamics near a micellar surface: origin of the universal slow relaxation at complex aqueous interfaces. *Phys. Rev. Lett.*, 2002, **89**, 115505-1–4.
85. Bagchi, B., Water solvation dynamics in the bulk and in the hydration layer of proteins and self-assemblies. *Ann. Rep. Prog. Chem. Sect. C*, 2003, **99**, 127–175.
86. Jana, M. and Bandyopadhyay, S., Kinetics of hydrogen bonds in aqueous solutions of cyclodextrin and its methyl-substituted forms. *J. Chem. Phys.*, 2011, **134**, 025103-1–9.
87. Sarma, R. and Paul, S., The effect of pressure on the hydration structure around hydrophobic solute: A molecular dynamics simulation study. *J. Chem. Phys.*, 2012, **136**, 114510-1-10; Paul, S., Liquid–vapour interfaces of aqueous trimethylamine-N-oxide solutions: a molecular dynamics simulation study. *Chem. Phys.*, 2010, **368**, 7–13.
88. Steinel, T., Asbury, J. B., Corcelli, S. A., Lawrence, C. P., Skinner, J. L. and Fayer, M. D., Water dynamics: dependence on local structure probed with vibrational echo correlation spectroscopy. *Chem. Phys. Lett.*, 2004, **386**, 295–300; Asbury, J. B., Steinel, T., Kwak, K., Corcelli, S. A., Lawrence, C. P., Skinner, J. L. and Fayer, M. D., Dynamics of water probed with vibrational echo correlation spectroscopy. *J. Chem. Phys.*, 2004, **121**, 12431–12446.
89. Lawrence, C. P. and Skinner, J. L., Ultrafast infrared spectroscopy probes hydrogen-bonding dynamics in liquid water. *Chem. Phys. Lett.*, 2003, **369**, 472–477; Lawrence, C. P. and Skinner, J. L., Vibrational spectroscopy of HOD in liquid D_2O. II. Infrared line shapes and vibrational Stokes shift. *J. Chem. Phys.*, 2002, **117**, 8847–8854; Lawrence, C. P. and Skinner, J. L., Vibrational spectroscopy of HOD in liquid. III. Spectral diffusion, and hydrogen-bonding and rotational dynamics. *J. Chem. Phys.*, 2003, **118**, 264–272.
90. Corcelli, S. A., Lawrence, C. P. and Skinner, J. L., Combined electronic structure/molecular dynamics approach for ultrafast infrared spectroscopy of dilute HOD in liquid H_2O and D_2O. *J. Chem. Phys.*, 2004, **120**, 8107–8117; Corcelli, S. A., Lawrence, C. P., Asbury, J. B., Steinel, T., Fayer, M. D. and Skinner, J. L., Spectral diffusion in a fluctuating charge model of water.*J. Chem. Phys.*, 2004, **121**, 8897–8900.
91. Schmidt, J. R., Roberts, S. T., Loparo, J. J., Tokmakoff, A., Fayer, M. D. and Skinner, J. L., Are water simulation models consistent with steady-state and ultrafast vibrational spectroscopy experiments? *Chem. Phys.*, 2007, **341**, 143–157; Auer, B., Kumar, R., Schmidt, J. R. and Skinner, J. L., Hydrogen bonding and Raman, IR, and 2D-IR spectroscopy of dilute HOD in liquid D_2O. *Proc. Natl. Acad. Sci. USA*, 2007, **104**, 14215–14220.
92. Skinner, J. L., Auer, B. M. and Lin, Y.-S., Vibrational line shapes, spectral diffusion, and hydrogen bonding in liquid water. *Adv. Chem. Phys.*, 2008, **142**, 59–103.
93. Bakker, H. J. and Skinner, J. L., Vibrational spectroscopy as a probe of structure and dynamics in liquid water. *Chem. Rev.*, 2010, **110**, 1498–1517; Skinner, J. L., Following the motions of water molecules in aqueous solutions. *Science*, 2010, **328**, 985–986.
94. Rey, R., Moller, K. B. and Hynes, J. T., Hydrogen bond dynamics in water and ultrafast infrared spectroscopy. *J. Phys. Chem. A*, 2002, **106**, 11993–11996; Moller, K. B., Rey, R. and Hynes, J. T., Hydrogen bond dynamics in water and ultrafast infrared spectroscopy: a theoretical study. *J. Phys. Chem. A*, 2004, **108**, 1275–1289.
95. Mallik, B. S. and Chandra, A., Vibrational spectral diffusion in supercritical D_2O from the first principles: an interplay between the dynamics of hydrogen bonds, dangling OD groups and inertial rotation. *J. Phys. Chem. A*, 2008, **112**, 13518–13527.
96. Mallik, B. S., Semparithi, A. and Chandra, A., A first principles theoretical study of vibrational spectral diffusion and hydrogen bond dynamics in aqueous ionic solutions: D_2O in hydration shells of Cl^- ions. *J. Chem. Phys.*, 2008, **129**, 194512–15.
97. Liu, P., Harder, E. and Berne, B. J., Hydrogen-bond dynamics in the air–water interface. *J. Phys. Chem. B*, 2005, **109**, 2949–2955.
98. Benjamin, I., Theoretical study of the water/1,2-dichloroethane interface: Structure, dynamics, and conformational equilibria at the liquid–liquid interface. *J. Chem. Phys.*, 1992, **97**, 1432–1445.
99. Linse, P., Monte Carlo simulation of liquid–liquid benzene-water interface. *J. Chem. Phys.*, 1987, **86**, 4177–4187.
100. Michael, D. and Benjamin, I., Solute orientational dynamics and surface roughness of water/hydrocarbon interfaces. *J. Phys. Chem.*, 1995, **99**, 1530–1536.
101. Michael, D. and Benjamin, I., Molecular dynamics simulation of the water–nitrobenzene interface. *J. Electroanal. Chem.*, 1998, **450**, 335–345.
102. Chang, T. M. and Dang, L. X., Molecular dynamics simulations of CCl_4–H_2O liquid–liquid interface with polarizable potential models. *J. Chem. Phys.*, 1996, **104**, 6772–6783.
103. Benjamin, I., Molecular structure and dynamics at liquid–liquid interfaces. *Annu. Rev. Phys. Chem.*, 1997, **48**, 407–451.
104. Chandra, A., Dynamical behavior of anion–water and water–water hydrogen bonds in aqueous electrolyte solutions: a molecular dynamics study. *J. Phys. Chem. B*, 2003, **107**, 3899–3906.
105. Grimme, S., Accurate description of van der Waals complexes by density functional theory including empirical corrections. *J. Comput. Chem.*, 2004, **25**, 1463–1473; Semi-empirical GGA-type density functional constructed with a long-range dispersion correction. *J. Comput. Chem.*, 2006, **27**, 1787–1799.
106. Schmidt, J., Vande Vondele, J., Kuo, I.-F.W., Sebastiani, D., Siepmann, J. I., Hutter, J. and Mundy, C. J., Isobaric–isothermal molecular dynamics simulations utilizing density functional theory: an assessment of the structure and density of water at near-ambient conditions. *J. Phys. Chem. B*, 2009, **113**, 11959–11964.
107. Wang, J., Roman-Perez, G., Soler, J. M., Artacho, E. and Fernandez-Serra, M. V., Density, structure, and dynamics of water: The effect of van der Waals interactions. *J. Chem. Phys.*, 2011, **134**, 024516-1–10.

ACKNOWLEDGEMENTS. We thank the Department of Science and Technology, New Delhi for financial support. A.C. dedicates this work to his teacher and mentor Biman Bagchi on his 60th birthday.